# T-State Hemoglobin with Four Ligands Bound

M. C. Marden,* J. Kister, B. Bohn, and C. Poyart
*INSERM U299, Hôpital de Bicêtre, 94275 Le Kremlin Bicêtre, France*
*Received July 16, 1987; Revised Manuscript Received November 4, 1987*

ABSTRACT: Flash photolysis kinetics have been measured for ligand recombination to hemoglobin (Hb) in the presence of two effectors: bezafibrate (Bzf) and inositol hexakisphosphate (IHP). The combined influence of the two independent effectors leads to predominantly T-state behavior. Samples equilibrated with 0.1 atm of CO are fully saturated, yet after photodissociation they show only T-state bimolecular recombination rates at all photolysis levels; this indicates that the allosteric transition from R to T occurs before CO rebinding and that the allosteric equilibrium favors the T-state tetramer with up to three ligands bound. Since all four ligands bind at the rate characteristic for the T-state, the return transition from T to R must occur after the fourth ligand was bound. At 1 atm of CO, rebinding to the initial R state competes with the allosteric transition resulting in a certain fraction of CO bound at the rate characteristic for the R state; this fraction is greater the smaller the percentage dissociation. Under 1 atm of oxygen, samples are not more than 93% saturated and show mainly T-state kinetics. The results show that all four hemes can bind oxygen or CO ligands in the T structure. The fraction of the kinetics occurring as geminate is less for partially liganded (T-state) samples than for fully liganded (R-state) Hb.

A unique feature of the hemoglobin (Hb)[1] tetramer is the equilibrium between high ligand affinity (R) and low ligand affinity (T) forms. Reference to R and T states assumes a two-state framework (Monod et al., 1965); in reality, several states are observed when effectors or a range of pH is considered (Minton & Imai, 1974; Shulman et al., 1975; Kwiatkowski & Noble, 1982; Lee et al., 1988). The total number of thermodynamic states and their properties are not yet well defined. The present study indicates an additional set of properties for Hb when two effectors are present.

Since T state is generally the deoxy form, it is difficult to measure its ligand binding properties, especially with a technique such as flash photolysis which probes only hemes with ligands. Stripped hemoglobin is mainly in the R state with two or more ligands bound. The natural effector 2,3-diphosphoglycerate (DPG) shifts the equilibrium toward the T state; inositol hexakisphosphate (IHP) is an even stronger effector which competes with DPG for the same site. Recently a new effector, bezafibrate (Bzf), has been shown to favor the T state and to bind at a different site involving contacts mainly with the $\alpha$ chains (Perutz & Poyart, 1983; Perutz et al., 1986). The combined use of these effectors shifts the equilibrium toward the T state, beyond that observed with either effector alone.

A recent claim based on oxygen equilibrium measurements (Di Cera et al., 1987) maintains that the T state cannot accept more than two ligands. The authors supported their claim with data of X-ray analysis of oxygenated Hb crystals showing only two ($\alpha$ chain) ligands bound (Brzozowski et al., 1984). This implies that a T to R transition must occur with at most two ligands bound and triply liganded Hb exists only in the R state. The present kinetic results using two effectors show evidence of T-state Hb with three and four ligands and are therefore a counterexample to this restriction. Fully ligated T state has also been reported for Hb Kansas with IHP and for HbA with IHP when NO is the ligand (Shulman et al., 1975). The different experimental results may indicate that binding three or four ligands to the T state is permitted in solution but not observed in the crystalline environment (Shibayama et al., 1986; Perutz et al., 1987).

Addition of both IHP and bezafibrate (Bzf) to hemoglobin independently favors low-affinity allosteric states of hemoglobin. The oxygen equilibrium curves at pH <7 indicate that the combination of these two effectors results in a shift toward lower affinity of both asymptotes of the binding curve resulting in an incomplete saturation, even under 1 atm of oxygen (unpublished results).

We report here flash photolysis studies of Hb with the ligands oxygen and CO. The additional amount of T-state material is evident, confirming the equilibrium measurements. Kinetic results show that both the bimolecular association (ON) rates and the allosteric equilibrium are changed when either IHP or Bzf is present. The data indicate that even with three CO ligands bound equilibrium favors the T-state Hb tetramer. This condition makes it possible to study T-state ligand binding and dissociation processes that were previously difficult to observe.

## Materials and Methods

Hb A was prepared from fresh red blood cell hemolysate by chromatography on a DEAE-Sephadex column. The purity of the solute was verified by isoelectric focusing, showing a single band migrating at p$I$ = 6.95. The Hb was further stripped of remaining contaminants on an ion-exchange column consisting of ion retardation resin AG11A8 and mixed-bed resin AG501X8-D (Bio-Rad). Hb was concentrated under vacuum and stored in the oxy form in liquid nitrogen.

For the flash photolysis experiments, the heme concentration was 30–100 $\mu$M in 10 mM HEPES buffer. Bezafibrate (Bzf), $M_r$ 361.5, was a gift of Laboratoire LIPHA (Lyon, France). Stock solutions of Bzf and IHP (Sigma) were prepared in the same buffer. Final concentrations were 1–3 mM Bzf and 1 mM IHP. For Hb-CO, the Hb solutions were first deoxygenated under a stream of humidified argon and then equilibrated with CO. No difference in absorption spectrum was observed for 1 or 0.1 atm of CO, indicating that the Hb is still

[1] Abbreviations: Hb, hemoglobin; HEPES, *N*-(2-hydroxyethyl)-piperazine-*N*′-2-ethanesulfonic acid; Bzf, bezafibrate, 2-[4-[2-[(4-chlorobenzoyl)amino]ethyl]phenoxy]-2-methylpropionic acid.

0006-2960/88/0427-1659$01.50/0 

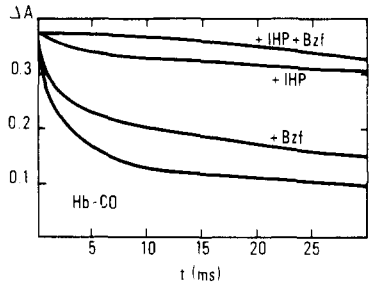


FIGURE 1: Bimolecular recombination kinetics of CO to hemoglobin (Hb, lowest curve), Hb + bezafibrate (Bzf), Hb + IHP, and Hb + Bzf + IHP. All samples are at pH 7, 10 mM HEPES buffer, 20 °C, 0.1 atm of CO. The increase in slow phase upon addition of effectors implies an increase in T-state tetramer.

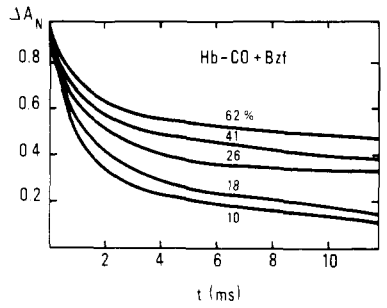


FIGURE 2: Bimolecular kinetics of CO to Hb + Bzf at various levels of photolysis, pH 7, 20 °C, 0.1 atm of CO. The curves were renormalized (each curve starts at 1) to show the changing fraction of the two kinetic phases with the percent dissociated. Less slow component (T state) is observed at lower photolysis levels.

fully saturated at 0.1 atm of CO. No sodium dithionite was added, since the fraction of met-Hb was determined to be less than 1% (CARY 219 spectrophotometer) and dithionite may increase the fraction dimer (Sawicki & Gibson, 1981).

Photodissociation was performed with a 10-ns laser (Quantel YG 585) delivering 160 mJ at 532 nm. The laser energy was varied to study the kinetics at partial dissociation.

Samples were studied in cuvettes of 1- or 2-mm optical path length. The detection beam at 436 nm was nearly collinear with the photolysis beam. The transmitted light intensity was detected with a photomultiplier (1P28, Hamamatsu, Japan) and recorded on a digital oscilloscope (LeCroy 9400). Data were transferred to an IBM microcomputer for calculation of absorbance changes and further data analysis. The entire 32K memory of the Lecroy oscilloscope was not read. For more efficient storage of the data, 2000 points were read, including 200 points before the flash to be used as the base line. The 2000 points were further reduced in a quasi-logarithmic fashion, keeping all the data just before and after the flash and progressively doubling the number of points averaged. An additional 10 segments of memory after the flash were read and averaged; these averaged points were logarithmically spaced. In this way the entire range of memory was covered, while reducing the kinetics to 130 data points.

Kinetic simulations were based on the two-state allosteric model, involving 10 tetrameric substates $R_i$,$T_i$, where $i$ is the number of ligands bound (0–4). $L$ is the allosteric equilibrium coefficient for deoxy T and R tetramers, and the equilibrium shifts by a factor $c$ (the ratio of T-state to R-state ligand affinities) for each ligand bound:

$$L = T_0/R_0 \qquad T_i/R_i = Lc^i \tag{1}$$

With the inclusion of dimers ($D_0$, $D_1$, and $D_2$), a total of 13 substates is required. Dimers were assigned the R-state bimolecular rates. The initial condition is the binomial distribution of states for a given fraction dissociation. The kinetics are then simulated in an iterative manner with explicit rates for all transitions: association (on) rates for the R and T states and 10 allosteric transition rates between R,T pairs. In analogy with the shift in equilibrium by the factor $c$, the R to T transition rates were assumed to decrease by a fixed factor $d$ for each ligand bound:

$$k_{R_i-T_i} = (1/d^i)k_{R_0-T_0} \tag{2}$$

(Sawicki & Gibson, 1979).

## RESULTS

Flash photolysis kinetics of the bimolecular recombination of CO to Hb are shown in Figure 1. The curves show the characteristic biphasic kinetics for the Hb tetramer, with rapid recombination to the high-affinity R state and the slow phase representing T-state recombination. The fraction occurring as the slow phase depends on the R–T equilibrium, the percentage of ligands dissociated, and the ligand concentration. The data in Figure 1 are for 70% ligand dissociation at the start of the bimolecular phase.

The full equilibrium amount of T-state material is formed after the flash only if the R to T transition is rapid compared to ligand recombination to the R state. This condition is satisfied for samples equilibrated with 0.1 atm of CO, which is sufficient for complete saturation before the flash. The data in Figure 1 therefore represent the difference in the allosteric equilibrium, the larger fraction of slow phase indicating a shift toward the T state.

The curves in Figure 1 show how the effectors increase the transient amount of T-state tetramers. The curve with the least amount of slow phase is for Hb without effector. Addition of NaCl shows a small increase in the fraction of slow phase (not shown). Bzf alone shows a substantial increase but still small compared to the effect of IHP alone. The combined effectors Bzf and IHP produce the maximum amount of T state.

Results with Bzf as the only effector are shown in Figure 2. To probe the R–T equilibrium at the various ligation levels, the photolysis energy was changed to vary the fraction dissociated, which changes the initial distribution of R states (Gibson, 1959; Sawicki & Gibson, 1976). At the highest laser energy (top curve in Figure 2), the main states produced by the flash are $R_0$ and $R_1$, and equilibrium favors the conversion to $T_0$ and $T_1$ which bind ligands at the slow T-state recombination. At sufficiently low photolysis levels, only the state $R_3$ is produced; if equilibrium heavily favors $R_3$ over $T_3$, the kinetics will show mainly the rapid R-state kinetics. The variation of the fraction occurring as slow phase is better seen by renormalizing each kinetic trace to the same initial level, as shown in Figure 2. The family of curves shows the characteristic decrease in the fraction of slow phase at decreasing photolysis levels.

The bimolecular recombination kinetics of CO to Hb at pH 6.5 with both Bzf and IHP bound are shown in Figure 3. The data at 0.1 atm of CO (upper portion) show only T-state kinetics, even at the lowest photolysis levels where triply liganded tetramer is the main form produced by the photolysis pulse. The fraction of slow phase depends on pH; at least 90% slow was observed at pH <7. All partially ligated states apparently convert to the T state. The dominant pathway is shown by the inset: photodissociation from $R_4$ to a distribution of partially liganded R states ($R_i$, $i$ = 0–3), then a transition from $R_i$ to $T_i$ followed by the slow ligand recombination in the T state, and finally a return to the initial state via $T_4$. The

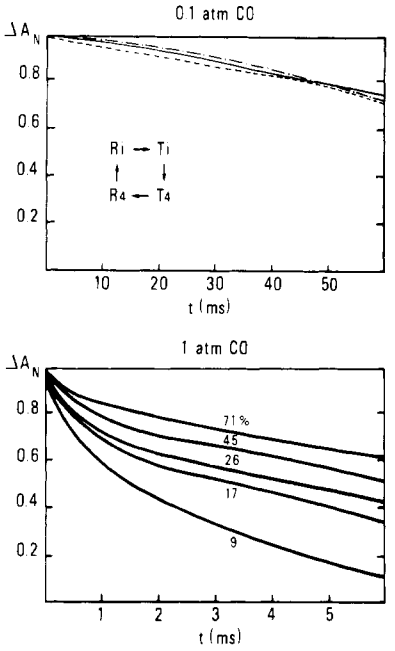


FIGURE 3: Bimolecular recombination kinetics of CO to Hb + Bzf + IHP at various photolysis levels, pH 6.5, 20 °C. At 0.1 atm of CO (upper portion), the kinetics show only the slow T-state behavior at all photolysis levels (9–70% shown). At 1 atm of CO (lower section), some rapid kinetics are seen, as the CO binding to the R state competes with the R to T transition. The presence of fast R-state kinetics implies that the sample is in the $R_4$ (not $T_4$) state before the flash. The lack of fast kinetics at 0.1 atm of CO suggests the main pathway (inset) is (1) dissociation of $R_4$ to $R_i$ ($i$ = 0–3), (2) transition from $R_i$ to $T_i$, (3) ligand recombination to T-state tetramer, and (4) return to the original state via $T_4$. At 1 atm of CO, the relative amplitude of the slow T phase decreases at lower dissociation levels, indicating that the R to T rate decreases with more ligands bound.

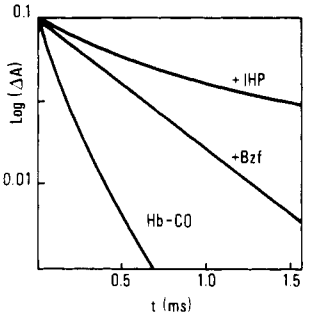


FIGURE 4: Bimolecular recombination of CO to Hb, Hb + Bzf, and Hb + IHP at pH 7, 10 mM HEPES buffer, 20 °C, 1 atm of CO. Curves are for partial dissociation which makes $R_3$–$R_4$ the dominant reaction.

highest dissociation levels showed at least 98% slow phase, which indicates that a small fraction of dimer was present.

At 1 atm of CO (Figure 3, lower portion) the rebinding to the initial R states is fast enough to compete with the allosteric transition resulting in an appreciable fraction for the rapid R-state recombination. A lower fraction of slow phase was observed at lower dissociation levels. The curves in Figure 3 were renormalized so that each curve starts from the same point in order to show the variation in the fraction slow.

The R- and T-state on rates decrease when effector is added. The R-state kinetics of CO recombination are shown in Figure 4 for Hb without and with Bzf or IHP. Both effectors decrease the R on rate by over a factor of 4 and induce biexponential kinetics, as previously observed for IHP (Gray & Gibson, 1971). The T-state on rates decreased by a factor of 1.7. A further decrease in on rate when both effectors are used was observed only for the T state.

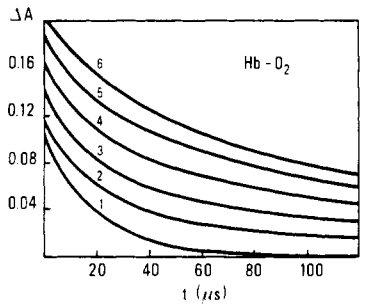


FIGURE 5: Bimolecular recombination kinetics of oxygen to Hb at pH 7, 1 atm of $O_2$, 20 °C. Curve 1 is stripped Hb; curves 2–6 are for Hb + Bzf at IHP to Hb ratios of 0, 1/4, 1/2, 3/4, and 1. For Hb with Bzf + IHP, the hemes are not fully saturated. Addition of effectors caused a decrease in the on rate and an increase in the yield for the bimolecular phase.

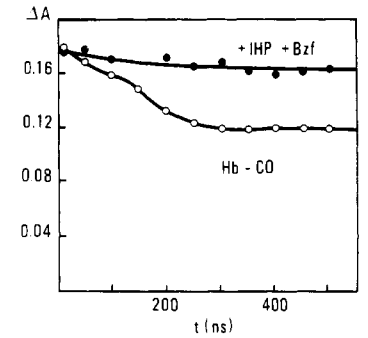


FIGURE 6: Geminate recombination of CO to Hb at pH 7, 20 °C. The lower curve showing 40% geminate recombination (O) is for fully saturated (R state) Hb without effector. The upper curve is for partially liganded Hb + Bzf + IHP and shows less than 10% geminate phase.

Samples of Hb with IHP and Bzf equilibrated with 1 atm of oxygen are only about 93% saturated at pH 7 (unpublished results). Data in Figure 5 show bimolecular kinetics for samples equilibrated with 1 atm of oxygen; Hb without effector had the smallest quantum yield and largest rate. Addition of Bzf caused a reduction in rate and an increase in the yield for the bimolecular phase. A further increase in yield was observed upon progressive addition of IHP.

The flash kinetics consist of a geminate (nanosecond) phase for ligands remaining near the iron atom and a bimolecular (millisecond) phase for ligands which have diffused into the surrounding solution. The larger quantum yield for the bimolecular phase in the presence of effector implies a smaller geminate reaction. Figure 6 shows the geminate recombination of CO at full and partial saturation. The lower curve was for fully liganded Hb without effector (R state). The laser energy was reduced to avoid multiple dissociation; the kinetics show 40% geminate phase. A second sample (top curve) with Bzf and IHP was equilibrated with CO to approximately half-saturation, to maintain a high proportion of T state. The saturation level was determined on a CARY spectrophotometer. The laser energy was adjusted to provide the same signal size as for the first sample; the kinetics show less than 10% geminate phase.

## Discussion

The kinetic results confirm the conclusions based on equilibrium measurements that the combined effects of IHP and Bzf shift the allosteric equilibrium toward the T state more than that obtained with either effector alone. The CO rebinding kinetics indicate that the T-state tetramer is dominant with up to three ligands bound and that the T state with four ligands is an intermediate state for returning to the stable R

form. This makes certain properties of the T state more easily observable than under ordinary conditions where the R state is favored.

*Association Rates.* A decreased on rate is mainly responsible for the lowered affinities in the presence of both IHP and Bzf. The R-state on rate was observed at low dissociation levels (forming mainly $R_3$) and high ligand concentration, which minimizes the R to T transition. In the presence of both effectors, the R-state on rate decreased by a factor of 6 for CO and a factor of 9 for oxygen. A decrease in rate of a factor a 5 for CO and 7 for oxygen upon addition of IHP was previously reported (Gray & Gibson, 1971). Use of both effectors apparently causes no additional change in the R-state on rate compared to use of IHP alone. The T-state on rate, observed at low CO and high dissociation levels, decreased by a factor of 1.7 for Bzf, 2 for IHP, and 3 in the presence of both effectors.

*Allosteric Equilibrium.* In the presence of both IHP and Bzf at 0.1 atm of CO, only the slow phase is observed (Figure 3, top), even at photolysis levels below 10%. This implies that the T state is favored with as many as three ligands bound. It can then be questioned whether the tetramer is in the R state with four ligands bound; if not, then the kinetics are explained simply as Hb being in the T state before and after the flash. Results at 1 atm of CO (Figure 3, bottom) show that CO rebinding to an initial rapid state competes with the allosteric transition. Rapid rates are observed at high CO concentrations, indicating that two allosteric forms exist and that the tetramer with four ligands bound is in the R state. At lower CO concentrations, which permits completion of the R to T transition after photolysis, all ligands bind at the T-state rate.

When ligands bind to deoxy-Hb, without effectors, the T to R transition occurs after two or three ligands are bound, resulting in an acceleration of the kinetics during the reaction. This increase in rate as the tetramer becomes saturated also implies that the rapid R-state on rate should be observed at low partial photolysis. Neither are observed for Hb with the combined effectors Bzf and IHP at 0.1 atm of CO, indicating that all four ligands bind at the T-state rate and the dominant pathway (inset on Figure 3) is a return to the R state via $T_4$.

*Geminate Recombination.* The results (Figure 6) show that a lower fraction of the recombination occurs as geminate for samples with effectors at low ligand saturation (T state) than for saturated samples without effector. This effect was inferred from the increased yield of the bimolecular phase by Sawicki and Gibson (1979) and Morris and Gibson (1984) and directly observed with double-flash or flow-flash techniques by Marden et al. (1987). Without effector, these experiments require a very low ligand saturation to maintain a nearly pure T state; however, the flash signal is then small since unliganded hemes provide no signal. Higher saturation levels can be used, but separation of the R and T contributions is then model dependent. Since the flash signal arises only from liganded hemes, the relevant quantity is the fraction of liganded hemes in the T state (and not total heme in the T state).

The increase in bimolecular yield is correlated with the decrease in on rate, whether effectors, different ligands, or comparison of the R- and T-state yields is being considered. This result is consistent with models using a linear sequence of barriers, such as the multiple barrier model of Austin et al. (1975). The bimolecular yield is determined by the competition between direct (geminate) rebinding and the ligand diffusion out to the solvent. A decrease in the geminate rate then implies a higher bimolecular yield (assuming no change in the diffusional steps). In a sequential model a lower geminate rate also slows down the overall on rate, since recombination occurs over the same barrier. This effect accounts for the lower bimolecular yields for dissociation of oxygen or NO due to their higher geminate rates. This effect is also observed in oxygen kinetics upon addition of effector (Figure 5).

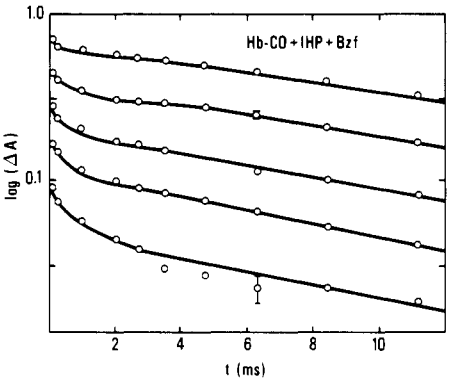


FIGURE 7: Simulation and kinetics of bimolecular rebinding of CO to Hb, pH 6.5, 20 °C, 1 atm of CO. Allosteric parameters were $L = 1.6 \times 10^8$ and $1/c = 200$, which favor the equilibrium $T_3/R_3$ by a factor of 20. The allosteric transition rate $R_0$ to $T_0$ was 50000 $s^{-1}$ with a factor $d = 4$ as the decrease in rate for each ligand bound. The association (on) rates were 1200 $s^{-1}$ for the R state and 65 $s^{-1}$ for the T state.

*R to T Rates.* For Hb with Bzf and IHP, the kinetics at 1 atm of CO show a decreasing fraction of slow bimolecular phase at lower photolysis levels (Figure 3). Since the data at 0.1 atm of CO show only the slow phase, the decrease in the fraction of slow phase at 1 atm of CO must be due to lack of time for the reequilibration: the CO rebinds to the R state before the R to T transition is complete. A larger fraction of fast phase is observed for a slower allosteric transition. Since the on rate is independent of saturation level, the rate of the R to T allosteric transition must decrease with more ligands bound.

This effect was directly observed at a wavelength isosbestic for the ligand dissociation (Sawicki & Gibson, 1979). They reported a decrease in the allosteric transition rate of a factor of $d = 2.4$ (per ligand bound) at 20 °C. The present results with two effectors could be simulated with values of $d$ from 2.5 to 4. The use of both effectors permits extending the measurements to the form with three ligands bound.

*Simulations.* The general conclusions drawn here require only a qualitative analysis. Specific parameters can be estimated under special conditions, for example, the rate from $R_3$ to $R_4$ at low dissociation levels where only $R_3$ is formed. In general, a distribution of initial states is involved, and a more detailed analysis requires a complete simulation.

Kinetic simulations using a two-state model are shown in Figure 7 for Hb-CO (1 atm of CO) with both IHP and Bzf, pH 6.5, 20 °C. All ten substates are considered. For these extreme conditions the allosteric parameters are not well determined. Many combinations of $L$ and $c$ can be used which favor the T state with three ligands bound and the R state with four ligands. For this extreme case, the data show over 92% slow phase at 0.1 atm of CO and 42% at 1 atm of CO (low dissociation levels), implying a minimum value of $1/c$ of about 50. Oxygen equilibrium data in the presence of effectors have a similar problem in determining all the parameters but indicate values of $1/c$ in excess of 200 (Shulman et al., 1975). For the present calculations a value of 200 was used with $L = 1.6 \times 10^8$. The R to T transition rates were assumed to decrease by a fixed factor $d$ for each ligand bound (Sawicki & Gibson, 1975); values of $d$ between 2.5 and 4 gave ac-

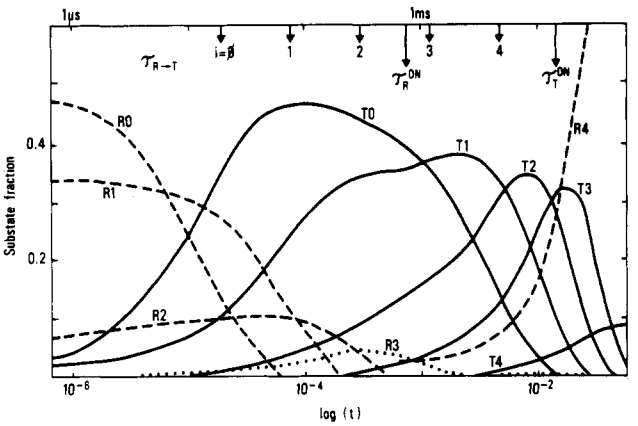


FIGURE 8: Simulation of the substates for the parameters used to generate the kinetics shown in Figure 7. For 85% dissociation the dominant species just after the flash are $R_0$ and $R_1$, which form $T_0$ and $T_1$ on the microsecond time scale; some $R_2$ and $R_3$ is formed under these conditions (1 atm of CO). The dominant reaction path is $R_0$–$T_0$–$T_1$–$T_2$–$T_3$–$T_4$–$R_4$; some ligands will branch at $T_3$–$R_3$–$R_4$. Final substates are the preflash values of 91% $R_4$ and 9% $T_4$.

ceptable simulations. With $d = 4$ a rate for $R_0$ to $T_0$ of 50000 $s^{-1}$ was required for simulations with an R on rate of 1200 $s^{-1}$ and a T on rate of 65 $s^{-1}$.

The vertical axis is logarithmic, which expands the plot at small values. The most significant deviations from the model are not the obvious misfit of the lowest curve near 5 ms (1% error) but points near 1 ms at most dissociation levels, which show the simulated curve leading the data. This is because a single R-state on rate was used, while a biexponential is observed in the presence of effector. Overall, the simulations are consistent with the two-state model but are not a stringent test of the model.

Figure 8 shows the substate populations for the set of parameters used to simulate the data of Figure 7. The time scale is logarithmic to include the initial R to T transition as well as the subsequent recombination to the T state. A dissociation of 85% was chosen for this example, since lower values show less deoxy form and the curves are more difficult to separate visually. The preflash conditions are 91% $R_4$ and 9% $T_4$; just after the flash a binomial distribution of substates provides the initial values for the kinetics. The R substates convert to T with the time constants marked at the top (number of ligands bound are given). There is some R-state recombination with these parameters resulting in an initial increase in the fraction of $R_2$ and $R_3$. Once the T state is formed there is the cascade $T_0$–$T_1$–$T_2$–$T_3$–$T_4$ before returning to $R_4$. Some ligands will follow the path $T_3$–$R_3$–$R_4$ with rate equal to

$$\lambda = k_{T_3 \rightarrow R_3} k_{on}^R / (k_{on}^R + k_{R_3 \rightarrow T_3}) \quad (3)$$

The rate for this path, which avoids $T_4$, may be larger or smaller than the T-state on rate. At low [CO], when $k_{R_3-T_3} \gg k_{on}^R$, the rate is the normal R-state on rate reduced by the equilibrium factor $R_3/T_3$. For the opposite condition, the reaction $T_3$ to $R_3$ is the limiting step. Without effectors, the return via $R_3$ or even $R_2$ is favored, and an acceleration is observed. With the present parameters, the return via $T_4$ is slightly favored. If the state $T_4$ were forbidden, the kinetics would show a delay for binding the last ligand.

The final process is a return to the initial preflash conditions. The amount of $T_4$ shown is rather arbitrary; a larger value of $1/c$ will reduce the equilibrium amount of $T_4$. As mentioned previously, this parameter is not well determined.

*Oxygen Recombination.* The oxygen data are more difficult to interpret than results with CO as ligand. The kinetics are independent of the fraction photolyzed, indicating that a single allosteric state is observed. The on rates become biphasic and may be similar for the two allosteric states in the presence of IHP and Bzf. There is therefore less information to describe the allosteric equilibrium. As with CO, the R-state on rates decrease upon addition of effector.

*Definition of R and T.* The addition of effectors to Hb results in new states, distinct from the original R and T states. This raises the question of how to define the R and T states. If the effectors changed only the allosteric equilibrium rather than properties of the two states, there would be no problem in distinguishing an R from a T state—for example, by the ligand affinity, the on rate, NMR spectra (Viggiano & Ho, 1979), X-ray structure, or the fraction of geminate recombination. However, the ligand affinity and rebinding rates in the presence of effector are not the same as either the original R or the T state (in the absence of effectors). The equilibrium in the presence of effectors therefore involves two new states: R′ and T′ (Kister et al., 1987) or some other notation describing the Hb–effector system. The problem is especially apparent when the high-affinity state of Hb with Bzf and IHP is considered; the affinity and on rates of this R′ state are similar to those of the T state of Hb without effectors.

The allosteric states cannot be defined as liganded and deoxy, since transients such as deoxy R can be formed by photodissociation. Different experimental procedures also produce inconsistent answers: the relaxation to T-like ligand binding kinetics occurs on the microsecond time scale, while UV Raman studies have reported a <7-ns relaxation of aromatic residues (possibly from the $\alpha$-1–$\beta$-2 contact) to a T-like state (Dasgupta et al., 1986). Thus, different parts of the protein may complete the relaxation at different times.

In conclusion, the combined influence of the effectors Bzf and IHP produces an allosteric equilibrium shifted toward the lower affinity form. The new T state has a lower on rate and affinity than those of the T state for Hb without effector. The new R state is similar in affinity and on rate to the T state of Hb without effector. The bimolecular recombination data with CO clearly show two phases whose proportion can be changed by varying the [CO] or percent dissociation. The data with CO as ligand indicate that the allosteric equilibrium favors the T state for triply liganded Hb and that quadruply liganded T state occurs as a transient state.

## ACKNOWLEDGMENTS

We thank Professor M. F. Perutz for a critical reading of the manuscript.

**Registry No.** Hb A, 9034-51-9; Bzf, 41859-67-0; IHP, 83-86-3; $O_2$, 7782-44-7; CO, 630-08-0.

## REFERENCES

Austin, R. H., Beeson, K. W., Eisenstein, L., Frauenfelder, H., & Gunsalus, I. C. (1975) *Biochemistry 14*, 5355–5373.

Brzozowski, A., Derewenda, Z., Dodson, E., Dodson, G., Grabowski, M., Liddington, R., Skarzynski, T., & Vallely, D. (1984) *Nature (London) 307*, 74–76.

Dasgupta, S., Copeland, R. A., & Spiro, T. G. (1986) *J. Biol. Chem. 261*, 10960–10962.

Di Cera, E., Robert, C. H., & Gill, S. H. (1987) *Biochemistry 26*, 4003–4008.

Gibson, Q. H. (1959) *Biochem. J. 71*, 293–303.

Gray, R. D., & Gibson, Q. H. (1971) *J. Biol. Chem. 246*, 7168–7174.

Kister, J., Edelstein, S. J., & Poyart, C. (1987) *Biophys. J. 52*, 527–535.

Kwiatkowski, L., & Noble, R. (1982) *J. Biol. Chem. 257*, 8891–8895.

Lee, A. W., Karplus, M., Poyart, C., & Bursaux, E. (1988) *Biochemistry* (in press).
Marden, M. C., Hazard, E. S., Kimble, C., & Gibson, Q. H. (1987) *Eur. J. Biochem. 169*, 611-615.
Minton, A. P., & Imai, K. (1974) *Proc. Natl. Acad. Sci. U.S.A. 71*, 1418-1421.
Monod, J., Wyman, J., & Changeux, J.-P. (1965) *J. Mol. Biol. 12*, 88-118.
Morris, R., & Gibson, Q. H. (1984) *J. Biol. Chem. 259*, 365-371.
Perutz, M. F., & Poyart, C. (1983) *Lancet*, 881-882.
Perutz, M. F., Fermi, G., Abraham, D. J., Poyart, C., & Bursaux, E. (1986) *J. Am. Chem. Soc. 108*, 1064-1078.
Perutz, M. F., Fermi, G., Luisi, B., Shaanan, B., & Liddington, R. C. (1987) *Acc. Chem. Res. 20*, 309-321.
Sawicki, C., & Gibson, Q. H. (1976) *J. Biol. Chem. 251*, 1533-1542.
Sawicki, C., & Gibson, Q. H. (1979) *J. Biol. Chem. 254*, 4058-4062.
Sawicki, C., & Gibson, Q. H. (1981) *Biophys. J. 35*, 265-270.
Shibayama, N., Morimoto, H., & Kitagawa, T. (1986) *J. Mol. Biol. 192*, 331-336.
Shulman, R. G., Hopfield, J. J., & Ogawa, S. (1975) *Q. Rev. Biophys. 8*, 325-420.
Viggiano, G., & Ho, C. (1979) *Proc. Natl. Acad. Sci. U.S.A. 76*, 3693-3677.

# Comparing the Polarities of the Amino Acids: Side-Chain Distribution Coefficients between the Vapor Phase, Cyclohexane, 1-Octanol, and Neutral Aqueous Solution†

Anna Radzicka and Richard Wolfenden*
*Department of Biochemistry, University of North Carolina, Chapel Hill, North Carolina 27514*
*Received May 26, 1987; Revised Manuscript Received September 29, 1987*

ABSTRACT: To obtain an indication of the tendencies of amino acids to leave water and enter a truly nonpolar condensed phase, distribution coefficients between dilute solution in water and dilute solution in wet cyclohexane have been determined for each of the common amino acid side chains at pH 7; they are found to be closely related to the inside–outside distributions of the side chains observed in globular proteins. There was no evidence that excess water enters cyclohexane in association with these solutes. Cyclohexane-to-water distribution coefficients can be combined with vapor-to-water distribution coefficients reported earlier to yield vapor-to-cyclohexane distribution coefficients. Vapor-to-cyclohexane distribution coefficients provide an experimental index of susceptibility to attraction by dispersion forces, and the corresponding free energies are found to be linearly related to side-chain surface areas. Observations using different solvents and variously substituted side chains suggest that alcohols such as 1-octanol exert a specific attraction on the side chain of tryptophan. When less polar phases are used as a reference, leucine, isoleucine, valine, phenylalanine, and methionine are found to be more hydrophobic than tryptophan.

When "molecular recognition" events occur in aqueous surroundings, solvent water must usually be displaced from the interacting groups. The solvation properties of amino acid side chains are of interest in attempting to understand the fidelity of activating enzymes in protein biosynthesis (Fersht & Kaethner, 1976) and to predict the biological activities of peptide analogues and mutant proteins. Solvation effects are also important in determining the structures of macromolecules, and the differential affinities of amino acid side chains for solvent water seem to constitute one of the stronger imperatives governing the structures of proteins in solution [for a comprehensive review, see Edsall and McKenzie (1983)]. For these reasons, there has been continuing interest in the differing solvation properties of amino acid side chains. Hydration potentials of amino acid side chains, representing their free energies of transfer from the vapor phase to neutral aqueous solution, have been found to be related to their outside–inside distributions in proteins, as indicated by earlier solvent accessibility calculations (Wolfenden et al., 1981). In a somewhat modified form, hydration potentials have been used to predict the portions of transmembrane proteins that are located within the lipid bilayer (Kyte & Doolittle, 1982). Distribution coefficients between water and hydroxylic solvents such as 1-octanol have also been found to be correlated with solvent accessibility in globular proteins (Fauchère & Pliska, 1983).

Different reference phases can be used to investigate the relative susceptibilities of amino acid side chains to different kinds of physical interaction. It is possible that any one of these phases might by coincidence approximate the environment experienced by a particular amino acid residue in some particular protein, but it also seems clear that no single reference phase is likely to serve as a general model for the interiors of globular proteins. For example, solutes in the dilute vapor phase are devoid of intermolecular contacts, whereas in the interior of a typical protein, there is little unoccupied volume, and dispersion and other attractive forces are at work. The solvation properties of hydroxylic organic solvents such as octanol are complicated by their ability to form specific hydrogen bonds to solutes and by the fact that they contain substantial concentrations of dissolved water. Thus, the

†Supported by Grant PCM-7823016 from the National Science Foundation.

0006-2960/88/0427-1664$01.50/0 